

Role of acid–base, redox and structural properties of VMgO catalysts in the oxidative dehydrogenation of propane

A. Pantazidis^a, A. Auroux^a, J.-M. Herrmann^b, C. Mirodatos^{a,*}

^a Institut de Recherches sur la Catalyse, C.N.R.S., 2, avenue Albert Einstein, F-69626 Villeurbanne Cédex, France

^b U.R.A. au C.N.R.S., 'Photocatalyse, Catalyse et Environnement', Ecole Centrale de Lyon, BP 163, F-69131 Ecully Cédex, France

Abstract

The oxidative dehydrogenation of propane was studied over VMgO catalysts in a wide range of V contents (5–45 wt%). The highest propene yields were observed for samples with low-to-medium V content. Electrical conductivity measurements demonstrated the presence of anionic vacancies, which participated to the redox catalytic cycle. The reoxidation step was shown to be rate limiting. Microcalorimetry measurements and DRIFT spectroscopy showed that an acid/base balance was equally required. Thus, the highest propene yields corresponded to adjusted redox potential combined with a strong Lewis acidity and a mild basicity. These observations, completed by the structural properties of the VMgO solids, led to the description of the active sites for the ODHP reaction.

Keywords: Acid–base properties; Redox properties; Structural properties; VMgO catalysts; Oxidative dehydrogenation of propane

1. Introduction

Magnesium vanadates are known to be efficient catalysts for the oxidative dehydrogenation (ODH) of light alkanes [1–4]. Patel and co-workers [1] attributed the higher selectivities observed on magnesium orthovanadate ($\text{Mg}_3\text{V}_2\text{O}_8$) to the presence of Mg–O–V bonds. These bridging units are assumed to be less readily reduced than the V–O–V units found in magnesium pyrovanadate ($\alpha\text{-Mg}_2\text{V}_2\text{O}_7$). By comparing the performances of various orthovanadates for the ODH of butane, the authors claimed that the easier the reducibility of V ions, the higher the combustion activity of the catalysts. On the contrary, Guerrero-Ruiz et al.

[2] proposed to relate the highest selectivities to propene obtained on the $\alpha\text{-Mg}_2\text{V}_2\text{O}_7$ phase with the high initial rate and level of reduction exhibited by this solid. They concluded that the easier the reduction of the catalyst, the higher its selectivity to propene. Valenzuela et al. [3] studied the effect of different additives on the performances of VMgO catalysts in ODH of propane and assumed a similar relationship between reducibility and selectivity to propene. Corma et al. [4] suggested that the incorporation of small amounts of V on a MgO surface modified not only the redox properties of the system but also the acid–base character of the oxygen species present on the catalyst surface, as revealed by shifts of XPS energies. These acid–base properties were related to the nucleophilic character of the lattice oxygen anions.

* Corresponding author.

In order to specify the parameters which actually control the catalytic performances of VMgO catalysts, a series of samples with various compositions and surface areas were prepared and thoroughly characterised. On the basis of the catalytic properties reported in [5], this paper focuses on the structural, acid–base and redox properties of the tested solids.

2. Experimental

2.1. Preparation method

The V-Mg-O catalysts were prepared by adding $\text{Mg}(\text{OH})_2$ to a hot aqueous solution of NH_4VO_3 [5]. Unless otherwise specified the samples were calcined at $T_c = 550^\circ\text{C}$ before characterization and/or reaction. The number placed before the formula V/VMgO corresponded to the weight percent of vanadium in the calcined sample.

2.2. Catalytic test

The catalysts (30 mg) were tested in a fixed bed micro-reactor at 500°C and atmospheric pressure. The reacting feed consisted of a $\text{C}_3\text{H}_8/\text{O}_2/\text{He} = 2.4/2.0/95.6$ mixture with a total flow rate of 58 ml/min.

2.3. Microcalorimetry

The samples were outgassed at 400°C for 15 h and placed in the microcalorimeter cell. Known amounts of probe adsorbates (NH_3 or SO_2) were admitted at 80°C until a final equilibrium pressure of 133.3 Pa was obtained. Above this pressure, the probe uptake increased very slowly as indicated by the adsorption isotherm and physisorption mainly occurred [6]. In order to evaluate the amount of irreversibly adsorbed probe ($V_{\text{ads,irr}}$), the sample was evacuated at 80°C after the first adsorption and a

second adsorption was performed at the same temperature. The irreversible chemisorption was determined by the difference between adsorption and readsorption isotherms at a pressure of 26.7 Pa [6]. Temperature-programmed reoxidations (TPO) were carried out in a heat flow differential scanning calorimeter coupled to a thermogravimeter (TG-DSC). The samples were first reduced under the reaction mixture $\text{C}_3\text{H}_8/\text{O}_2/\text{He}$ (4/2/94 vol%) flowing at 20 ml/min, raising the temperature to 600°C at $5^\circ\text{C}/\text{min}$. The samples were then reoxidised under O_2/He (43 vol%) under same flow rate and temperature ramp conditions.

2.4. Electrical conductivity

The electrical conductivity σ ($\text{ohm}^{-1} \text{cm}^{-1}$) was determined by the formula: $\sigma = (1/R)(h/S)$, where R is the measured electrical resistance (ohm), S the cross sectional area of the electrodes (cm^2) and h the catalyst bed thickness (cm). The partial pressure of oxygen and temperature were varied. All the samples behaved as semiconductors, with σ varying exponentially with T according to $\sigma_e = kP_{\text{O}_2}^{(1/n)} \exp(-E_c/RT)$, where E_c is the activation energy of conduction (kJ/mol). Reduction–reoxidation sequences were carried out at 500°C in the presence of the reaction mixture ($P_{\text{C}_3\text{H}_8} = 2.4 \text{ kPa}$, $P_{\text{O}_2} = 2.0 \text{ kPa}$), then of oxygen ($P_{\text{O}_2} = 2.0 \text{ kPa}$) and finally of propane ($P_{\text{C}_3\text{H}_8} = 2.4 \text{ kPa}$).

2.5. In situ diffuse reflectance Fourier transform infra-red spectroscopy (DRIFT)

The catalyst was loaded into an in situ DRIFT cell directly connected with the catalytic test set-up. The sample was pretreated under argon flow at increasing temperature ($5^\circ\text{C}/\text{min}$) up to 550°C , and cooled down to 80°C under argon flow. It was then exposed at consecutive pulses (0.03 ml) of basic (NH_3) or acidic (CO_2) probe molecules.

3. Results

3.1. Catalytic properties

As seen in Fig. 1, a maximum in propene yields was observed at a low V content (10–14 wt%) for given operating conditions. However, selectivity to propene exhibited a much lower sensitivity to V loading, remaining around 65–75% over a wide range of V content (12–45 wt%) [5].

3.2. Structural properties

All the slopes ($1/n$) of the various isotherms $\log \sigma = f(\log P_{O_2})$ were found to be negative (Fig. 2A), indicating that all samples behaved as n-type semiconductors [7,8]. Most of the samples presented a value of n between 4 and 6. Though the physical meaning of these values was not straightforward, it could correspond to a model of singly ($V_{O_2}^{1+}$) or doubly ($V_{O_2}^{2+}$) ionised anionic vacancies, respectively [7]. Fig. 2B (curve a) presents the effect of V content on electrical conductivity (σ) measured at 500°C under oxygen pressure. Unpromoted magnesia presented a high electrical conductivity, which decreased after V addition (almost two orders of magnitude) and remained more or less constant up to 30 wt% V. For higher V loading, σ

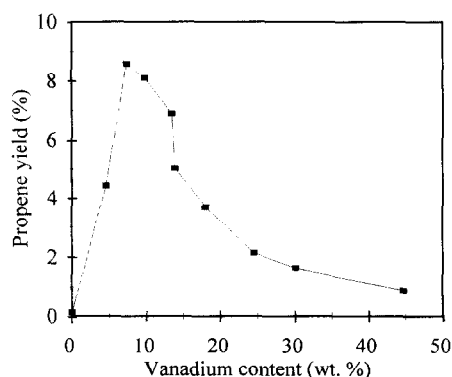


Fig. 1. Propene yield (%) of the VMgO catalysts as a function of vanadium loading.

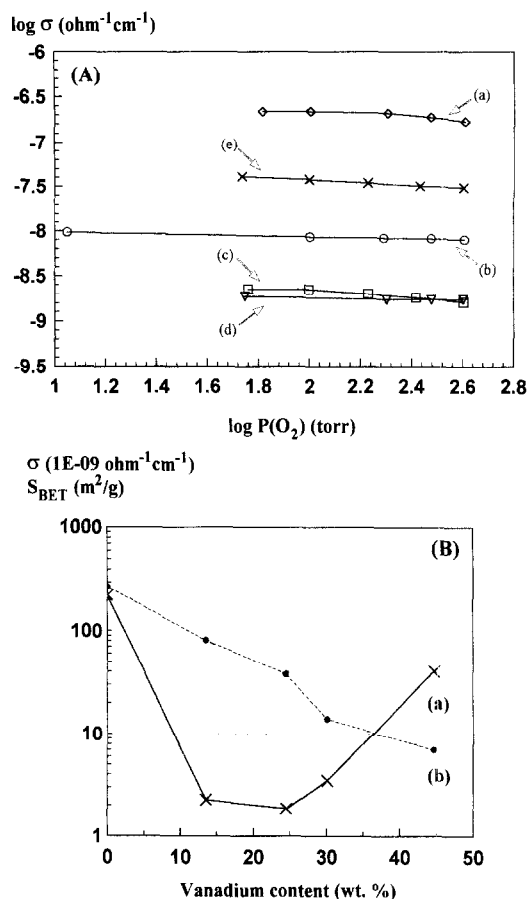


Fig. 2. (A) Variations of electrical conductivity (σ) with oxygen partial pressure for the (a) MgO, (b) 14V/VMgO, $T_c = 800^\circ\text{C}$, (c) 14V/VMgO, $T_c = 550^\circ\text{C}$, (d) the 25V/VMgO and the (e) 45V/VMgO samples. (B) Variations of σ (curve a) and BET surface area (curve b) with VMgO catalyst composition at 500°C under 6.7 kPa of O_2 .

increased again (one order of magnitude). The activation energy of conduction (E_c) was calculated from the slopes of the various curves $\log \sigma = f(1/T)$ at constant P_{O_2} . The E_c values were very close for the unpromoted magnesia and for the samples loaded with up to 30 wt% of V (≈ 140 kJ/mol). This indicated that for low and medium V content, the electrical conductivity, though considerably hindered after V addition, remained intrinsically of identical nature [7]. The E_c value decreased for the 45V/VMgO sample (104 kJ/mol), tending to a value characteristic for the metavanadate phase

[2]. A marked decrease in the BET surface area was equally observed after V addition (Fig. 2B, curve b). This effect could at least partially account for the observed drop in conductivity.

DRIFT investigations presented in [5], revealed that the unpromoted magnesia was strongly carbonated (mostly unidentate species). The surface was also partly hydroxylated (mainly basic OH groups). After promotion with vanadium the overall carbonate concentration decreased significantly, especially the unidentate species. The basic OH groups also decreased and two types of more acidic hydroxyl groups appeared. At large V content, only acid OH groups were detected while bidentate carbonate or, most likely, acid carbonate groups were observed [9].

3.3. Acid–base properties

The acid strength of the VMgO samples revealed by the differential heat of adsorption (Q , kJ/mol) vs. ammonia adsorption (V_{ads} , $\mu\text{mol}/\text{m}^2$) increased up to 14 wt% of V loading (Fig. 3A). For higher loading, the strong acidity decreased while weaker acid sites developed above 25 wt% V. This maximum in strong acidity observed for the 14V/VMgO sample was also outlined by plotting the initial differential heat of adsorption Q_{init} (kJ/mol) vs. V content (Fig. 4, curve c). In contrast, the total intrinsic acidity measured by irreversible NH_3 adsorption (Fig. 4, curve b) increased regularly over the range of V addition. Ammonia adsorption was also followed by in situ DRIFT spectroscopy (Fig. 5). Lewis-type ($\delta_{\text{as}}(\text{NH}_3)$ at 1597 cm^{-1} , $\delta_{\text{s}}(\text{NH}_3)$ at 1165 cm^{-1} and $\nu(\text{NH}_3)$ at 3276 cm^{-1}) and Brönsted-type acidity ($\delta_{\text{as}}(\text{NH}_4)^+$ at 1675 cm^{-1} , $\delta_{\text{s}}(\text{NH}_4)^+$ at 1434 cm^{-1} and $\nu(\text{NH}_4)^+$ at 3375 cm^{-1}) [9] were detected at low V loading (5V/VMgO, curve a). Mainly Lewis-type acidity (1603 cm^{-1} , 1178 cm^{-1} and 3274 cm^{-1}) was detected at higher V content (14V/VMgO, curve b). At higher V content (25V/VMgO, curve c), the intensity of the vibrations ascribed to Lewis sites decreased

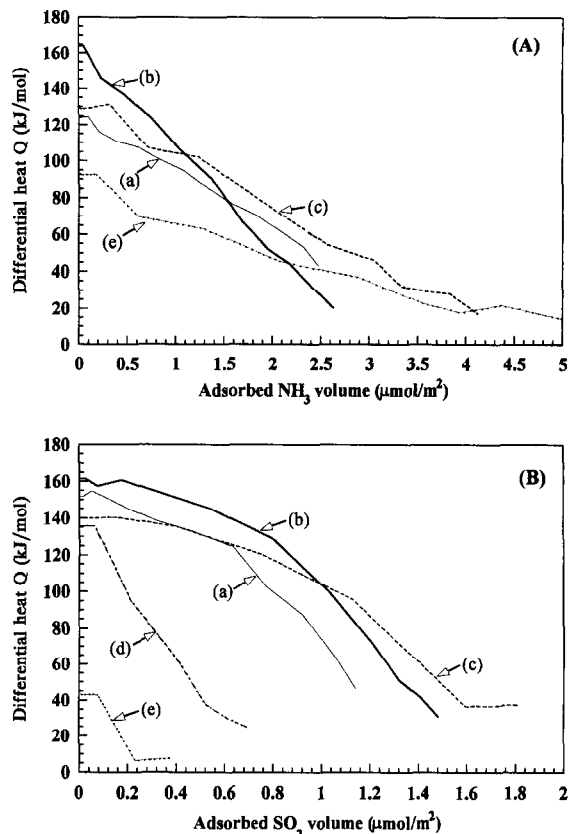


Fig. 3. Differential heat of (A) NH_3 and (B) SO_2 adsorption at 80°C vs. the probe uptake for the: (a) 5V/VMgO, (b) 14V/VMgO, (c) 25V/VMgO, (d) 30V/VMgO and (e) 45V/VMgO samples.

and vanished on the 45V/VMgO sample (curve d), which presented only Brönsted-type acidity (1117 cm^{-1} and 3174 cm^{-1}).

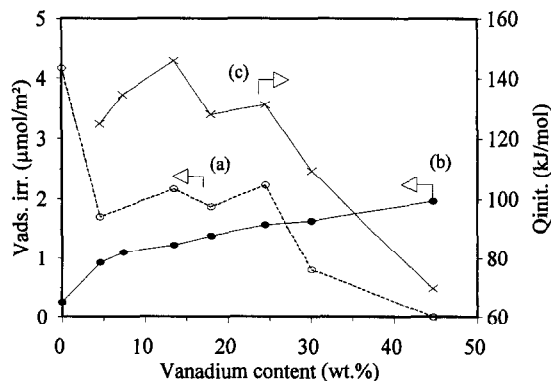


Fig. 4. Effect of V content on the irreversibly adsorbed (a) SO_2 , (b) NH_3 volume, and on the initial differential heat of NH_3 adsorption Q_{init} (c).

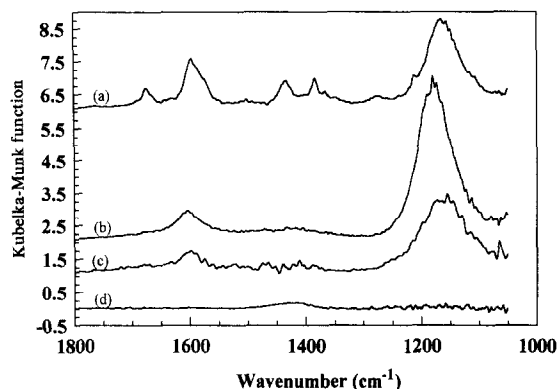


Fig. 5. DRIFT spectra recorded at 80°C under Ar flow after the 5th pulse of NH_3 for the: (a) 5V/VMgO, (b) 14V/VMgO, (c) 30V/VMgO and (d) 45V/VMgO samples.

The basicity of the VMgO samples measured by sulphur dioxide adsorption (Fig. 3B) remained unchanged for loading up to 25 wt% V. At higher loading, the basicity decreased to vanish on the 45V/VMgO sample. The intrinsic basicity measured by the amount of irreversibly adsorbed SO_2 per surface unit (Fig. 4, curve a) was found to markedly decrease from unpromoted to promoted magnesia, then to be stable up to 25 wt% V addition, then to decrease again and to vanish at very high V contents. Surface basicity was also investigated by carbon dioxide adsorption followed by in situ DRIFT spectroscopy. Pure MgO and low V content samples showed a strongly carbonated surface with the presence of unidentate, bidentate and free carbonates. As V content increased, the amount of unidentate species markedly decreased. Only bidentate carbonates were observed at 14 wt% V, while no CO_2 adsorption was observed on the 25V/VMgO and 45V/VMgO samples.

3.4. Redox properties

Kinetic measurements of electrical conductivity (σ) were carried out at 500°C in the presence of propane or under reaction conditions. Fig. 6 reports the data obtained for the 14V/VMgO sample calcined at 800 and 550°C (a and b) and for the 45V/VMgO sample calcined at 550°C (c). The electrical conductivity

was found to be very sensitive to variations of feed mixture. An increase in σ corresponded to a reduction phenomenon (release of free electrons available for conduction) and a drop in σ to a reoxidation phenomenon [7]. The slopes of the increasing or decreasing σ curves were related to the rate of reduction or reoxidation of the catalyst, respectively. Our main observations were the following: (i) σ increased by several orders of magnitude when propane or oxygen/propane mixture was introduced (reduction step), (ii) the lowest reduction level was obtained for the 14V/VMgO sample calcined at 800°C, (iii) the reduction level attained under propane (point C) was higher than under reaction mixture (point A) for the 14V/VMgO samples, (iv) the highest rate of reduction was observed for the 45V/VMgO sample, (v) a complete and fast reoxidation was observed for the 14V/VMgO samples, while the 45V/VMgO sample remained partially reduced and (vi) the rate of reoxidation of the 45V/VMgO sample was very slow.

TPO experiments were also performed in the TG/DSC set-up after in situ reduction under reaction mixture from 25 to 600°C. Weight gains (expressed as weight percentage and as atomic ratio of gained O atoms per total V

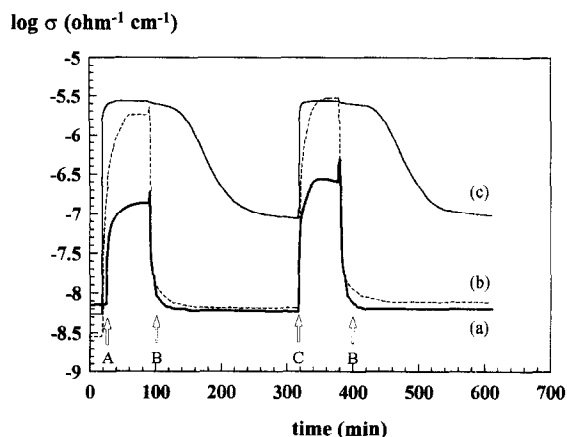


Fig. 6. Variation of electrical conductivity σ during redox sequences at 500°C on the (a) 14V/VMgO, $T_c = 800^\circ\text{C}$, (b) 14V/VMgO and (c) 45V/VMgO catalysts; initial atmosphere, oxygen; (A) reaction mixture; (B) vacuum, then oxygen; and (C) propane [5].

Table 1

Weight gain and heat release occurring during TPO from 25 to 600°C after reduction under oxygen/propane mixture

Catalysts	$\Delta m/m$ (%)	Atom O/ atom V	ΔH (kJ/atom V)
14V/VMgO	2.2	0.52	103
30V/VMgO	6.3	0.66	121

atom) and heat production (expressed in kJ per total V atom) due to catalyst reoxidation are summarised in Table 1.

For both catalysts, the vanadate phase was rather deeply reduced under reaction conditions and this reduction was reversible under TPO conditions. Within the uncertainty of the TG/DSC measurements, no major difference was noted between the two samples concerning the degree of reduction and the heat of oxidation. However, the TPO curves clearly indicated that the reoxidation process was slower on the high V content samples, in agreement with the observations obtained from electrical conductivity measurements.

4. Discussion and conclusions

The band gap energy value reported in literature for MgO is in the range of 8.7 eV and characterises an insulator rather than a semiconductor [10]. However, a high conductivity was measured on the present MgO sample (Fig. 2). This strongly suggests a preferential surface conductivity favoured by mobile adspecies. Indeed hydroxyl groups and surface carbonate or hydrogenocarbonates were detected by DRIFT spectroscopy and these adspecies were reported to favour electrical conductivity [7].

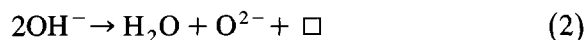
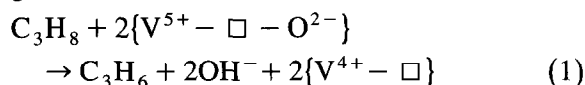
The addition of even low amounts of vanadium oxide to magnesia induced a considerable loss in electrical conductivity (Fig. 2). The electrical conductivity was shown however to remain of identical nature and most likely related to the magnesia phase up to 25 wt% V. Though significant, the loss of surface area observed after V addition (Fig. 2B) cannot explain by itself the almost two orders of magnitude de-

crease in electrical conductivity. The σ decrease would therefore also arise from the strong surface decarbonation and dehydroxylation observed by DRIFT upon V addition. The above confirms the assumption of an electrical conductivity essentially controlled by surface phenomena. Moreover, a thorough characterisation of the low V contents solids revealed the coexistence of the orthovanadate phase ($\text{Mg}_3\text{V}_2\text{O}_8$) with an excess of MgO [5].

For V contents higher than 25 wt%, major changes in catalyst structure were observed which corresponded to the development of pure VMgO phases: (i) the activation energy for conductivity decreased significantly and σ was shown to tend to a σ value characteristic for the pure magnesium vanadate phases (104 kJ/mol), (ii) XRD and ^{51}V NMR indicated that the pyrovanadate phase ($\alpha\text{-Mg}_2\text{V}_2\text{O}_7$) was dominant in the 30V/VMgO sample, while the metavanadate phase (MgV_2O_6) was present in the 45V/VMgO sample [5].

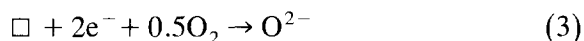
The high propene yields observed in the low-to-medium V range seem therefore to be related to mixed and inhomogeneous MgO/VMgO phases rather than to pure VMgO phases.

All the catalysts were shown to behave as n-type semiconductors following the model of anionic vacancies. Changes in electrical conductivity during reduction and reoxidation sequences (Fig. 6) revealed that a completely reversible redox capacity was required for active catalysts in ODHP. More precisely, the reoxidation step under oxygen flow (point B) appeared to be much slower and incomplete on the little active sample (45V/VMgO). Inversely, the reduction step which occurred under reacting mixture or under pure propane was fast in both cases, but even faster for high V contents. This reduction step, which led to propene formation even in the absence of oxygen [5], can be written as:



where \square are anionic vacancies required to accommodate the electrons which participate to the enhanced electrical conductivity. Actually, Eq. (1) would correspond to sequential steps including a first H abstraction from the secondary C, forming a propyl species followed by the β -elimination of a second H leading to propene desorption, as proposed in [1,5].

From the above, the reduction steps can hardly be considered as rate limiting within the catalytic redox cycle since the less active catalyst (45V/VMgO) was the easiest to reduce. In contrast, the reoxidation step was shown to be slow for the latter. This step, which actually would correspond to site regeneration according to:



could therefore be considered as rate limiting.

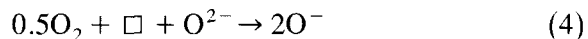
As discussed in [5], large polymeric units $(V-O-V)_n$ are formed on the catalyst surface for the case of high V contents. These defect free units would not favour the presence of anionic vacancies which are required for the active site regeneration. In contrast, at low-to-medium V content, isolated or corner linked VO_4^{3-} units in intimate contact with the MgO phase would form a defect rich surface structure. According to Eq. (3), this would favour the reduced site reoxidation and therefore explain the high catalytic activity of these samples.

At variance with the redox potential, no direct relationship between total acidity and activity was found since intrinsic acidity was shown to increase regularly over the range of active and selective samples (Fig. 4, curve b), while significant changes in intrinsic activity were noted. However, it was shown that the nature of the acid sites varied with V content. Strong acidity (Fig. 4c) presented a maximum at 14 wt% V where the best catalytic performances were achieved (Fig. 1a). This strong acidity was shown furthermore to be mainly Lewis acidity (Fig. 5b). In addition to strong acidity, a mild and constant basicity was also measured over the whole range of active catalysts (Fig. 5,

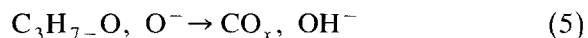
curve a). For high V content, no basicity was measured, which corresponded to less active and selective samples.

It can therefore be deduced that the most active and selective catalysts combine both a strong Lewis acidity and a mild basicity. Referring to the above equations describing the selective catalytic cycle, the required anionic vacancies could be considered as the actual Lewis centers being electron acceptors, while the lattice oxygen atoms which participate to the alkane C–H bond activation by forming OH groups ($V-O-V$, $V-O-Mg$ or $V=O$) would constitute the required surface basicity.

On the other hand, it was also proposed in [5] that acid/base pair sites would equally be involved in the non selective pathway. This would occur via the formation of O^- adspecies arising from the reaction of gaseous oxygen with surface according to:



These nucleophilic species would competitively attack the C atoms of propyl radicals to form propoxy intermediates, which would stepwise be transformed into acetate, carbonate or carboxylate and further on into combustion products according to:



It can be concluded that an acid/base balance is needed for good catalytic performances in ODHP. Too high basicity or absence of basicity favours the unselective route at the expenses of the selective one, as observed at very low or very high V contents, respectively. It could also interfere on the catalytic cycle via the surface dehydroxylation step (Eq. 2). In contrast, a mostly acidic surface without basicity would hinder key activation steps such as H abstractions and also propene desorption, as observed for very high V loadings.

To summarise, the highest propene yields were observed for samples with low-to-medium V contents (around 14 wt%). This composition would ensure the fast redox turn-over involved

in the propane-to-propene process. It also corresponds to a strong Lewis acidity and a mild basicity, which de facto may also be considered as a prerequisite for performing ODHP catalysts.

Acknowledgements

This work was supported by the EU network 'Euroxycat'.

References

- [1] M. Chaar, D. Patel and H. Kung, *J. Catal.*, 109 (1988) 463; D. Patel, P.J. Andersen and H.H. Kung, *J. Catal.*, 125 (1990) 132; H.H. Kung, *Adv. Catal.*, 40 (1994) 1.
- [2] A. Guerrero-Ruiz, I. Rodriguez-Ramos, J.L.G. Fierro, V. Soenen, J.M. Herrmann and J. C. Volta, in P. Ruiz and B. Delmon, Editors, *Novel Development in Selective Oxidation by Heterogeneous Catalysis*, Elsevier, Amsterdam, Vol. 72, 1992, p. 203.
- [3] R.X. Valenzuela, E.A. Mamedov and V. Cortes Corberan, *React. Kinet. Catal. Lett.*, 55 (1995) 213.
- [4] A. Corma, J. M. Lopez Nieto and N. Paredes, *J. Catal.* 144 (1993) 425.
- [5] A. Pantazidis and C. Mirodatos, *ACS Symp. Ser.*, *Heterogeneous Hydrocarbon Oxidation*, 1996, accepted; A. Pantazidis and C. Mirodatos, *Proc. 11th Int. Congr. Catalysis*, Baltimore, 1996, accepted.
- [6] A. Auroux, in B. Imelik and J. C. Védrine, Editors, *Catalyst Characterisation*, Plenum Press, New York, 1994.
- [7] J.-M. Herrmann, in B. Imelik and J. C. Védrine, Editors, *Catalyst Characterisation*, Plenum Press, New York, 1994.
- [8] Z. Zhang, X.E. Verykios and M. Baerns, *Catal. Rev.-Sci. Eng.*, 36 (1994) 507; Z. Zhang and M. Baerns, *J. Catal.*, 135 (1992) 317.
- [9] G. Socrates, *Infrared Characteristic Group Frequencies*, 2nd edn., Wiley, Chichester, 1980.
- [10] O. Krylov, *Catalysis by Non-metals: Rules for Catalyst Selection*, Academic Press, London, 1970.